ACS APPLIED MATERIALS & INTERFACES

Research Article

www.acsami.org

Breath Figure Patterns Made Easy

Chuixiu Huang,[†,§] Tripta Kamra,[‡] Shilpi Chaudhary,[‡] and Xiantao Shen*[,†,∥]

[†]G&T Septech, P.O. Box 33, N-1917 Ytre Enebakk, Oslo, Norway

[‡]Division of Synchrotron Radiation Research, Lund University, Box 118, 221 00 Lund, Sweden

[§]Department of Pharmaceutical Chemistry, School of Pharmacy, University of Oslo, P.O. Box 1068, Blindern, 0316 Oslo, Norway

[∥]Department of Pure and Applied Biochemistry, Lund University, P.O. Box 124, 22100 Lund, Sweden

Supporting Information

ABSTRACT: In this work, a simple breath figure method was proposed to directly fabricate large-area and ordered honeycomb structures on commercial PMMA substrates or PS Petri dishes without the use of an external polymer solution. The obtained honeycomb structure is indeed part of the substrate, providing the honeycomb layer with enough mechanical stability. The breath figure method in this work for the synthesis of honeycomb structure is extremely simple with scale-up capability to large-area production, which offers new insights into surface engineering with great potential in commercial technologies. For example, using the honeycomb-patterned Petri dishes prepared via this method, cells can be easily separated into divided aggregation, which favors understanding of naturally occurring networks in higher organisms and cell−cell and cell−matrix interactions, and the therapeutic control of genetic circuits.

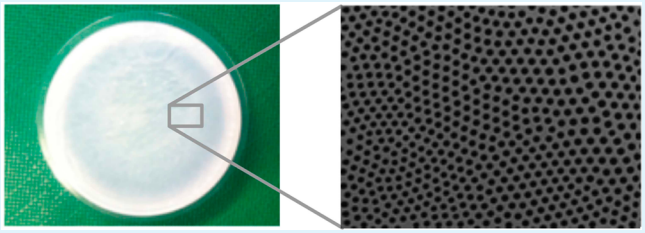

KEYWORDS: *breath figure, semidirect, honeycomb structures, Petri dish, cell aggregation*

INTRODUCTION

Polymeric films with well-ordered pores with a narrow size distribution are of great interest in industry for a variety of applications.[1,2] Several techniques for the formation of ordered porous polymeric films have been reported, including photolithography, soft lithography, and templating methods.[3,4] Among these approaches, the breath figure (BF) method has attracted attention as an alternative bottom-up way to generate honeycomb structures on micro- and nanoscales.[5−8] The key step in the traditional BF method involved stabilizing condensed water droplets on a polymer solution.[9,10] Typically, a polymer solution was first cast on a substrate under high humidity. During the evaporation of the solvent, the surface temperature of the solution was decreased, which caused the condensation of water as small droplets on the substrate.[11,12] The ordered water droplets then acted as an ordered template by self-assembly on the surface of the polymer solution, resulting in figures of honeycomb structures on the phase-separated polymer after the water had finally evaporated (Scheme S1a of the Supporting Information).[13,14] Via the control of the polymer composition, solvent, polymer concentration, casting volume, relative humidity, air flow, temperature, and substrates in the normal breath figure (NBF) technique, ordered holes in a hexagonal lattice might be created within a size range from 300 nm to 20 μm.[15,16] More recently, Farbod et al. reported a modified BF method to pattern breath figure on a substrate material without applying an external polymer solution (Scheme S1b of the Supporting Information).[17] This method was named direct breath figure (DBF). In this DBF process, a mixture of a good solvent (tetrahydrofuran) and a controlled amount of a nonsolvent (H_2O) was used to create directly porous structures on poly(methyl methacrylate) (PMMA) in a dry atmosphere. The main advantage of the DBF method is that the obtained figure was indeed part of the substrate. However, the honeycomb structure of the obtained figures was not ordered compared with that of the NBF method.

By combining the advantages of both NBF and DBF methods, we herein propose a new breath figure method for directly preparing honeycomb-structured substrates. Here, this new method is named semidirect breath figure (sDBF). During the synthesis, a pure solvent (chloroform) was used instead of an external polymer solution. When the substrate with chloroform was placed under a humid flow, the following steps were performed: (1) a cold surface formed by solvent evaporation, (2) water condensation on the solution, (3) arrangement of the water droplets with hexagonal packing, (4) swelling, dissolving, and drying of the surface polymer on the substrate material (in this process, the condensed water droplets served as templates for the honeycomb), and (5) total evaporation of the solvent and water to achieve a honeycomb structure on the substrate (Scheme 1).

It is noted that the simple breath figure method proposed here could be used to directly fabricate ordered honeycomb

Received: February 21, 2014
Accepted: April 1, 2014
Published: April 1, 2014

   dx.doi.org/10.1021/am501096k | ACS Appl. Mater. Interfaces 2014, 6, 5971−5976

Scheme 1. Representation of the Semidirect Breath Figure Method for the Preparation of Ordered Honeycomb Structures on Commercial Polymer Substrates

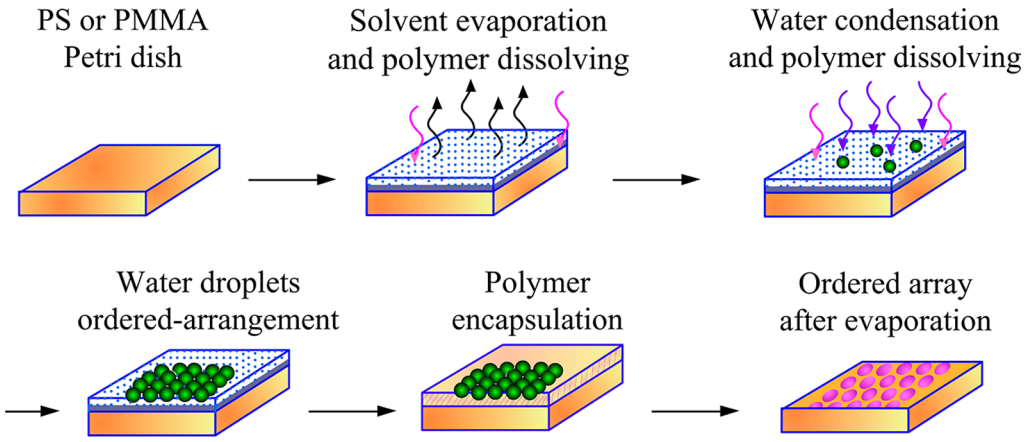

structures in the PS Petri dishes, which offers new insights into surface engineering with great potential in commercial technologies. As an example, cell attachment and cell growth on the honeycomb-patterned Petri dishes prepared under different humidity conditions (in comparison to a flat-bottomed PS Petri culture) were investigated, which would provide technical information for understanding naturally occurring networks in higher organisms.

EXPERIMENTAL PROCEDURES

Materials. Nunclon cell Petri dishes [polystyrene (PS; M_w ~ 220000), 3.5 cm in diameter] were purchased from Sigma-Aldrich. Poly(methyl methacrylate) (PMMA; M_w ~ 176000; 9 cm in diameter) Petri dishes were obtained from Shunda Supplies shop in Wuning of Dongyang City (China) and cut into rectangular plates (5 cm × 3 cm). Polystyrene (PS; average M_w of ~192000) was provided by Sigma-Aldrich.

Preparation of Honeycomb Structures Using the sDBF Method. A schematic representation of the experimental setup for the preparation of honeycomb structures is shown in Scheme 2. The carrier gas was bubbled through water, producing water vapor on the solution surface. The gas flow was controlled with a needle valve. A more detailed description of the techniques is available in ref 18. In a typical honeycomb structure synthesis process, 1 mL of chloroform was carefully cast onto a clean PS Petri dish or PMMA substrate. The commercial substrates were then immediately placed in a stream of water-saturated air. The humidity of the air flow was maintained at 75% by controlling the flow rate. After solidification for 30 min, the film was dried at room temperature.

Scheme 2. Representation of the Experimental Setup (adapted from ref 18)

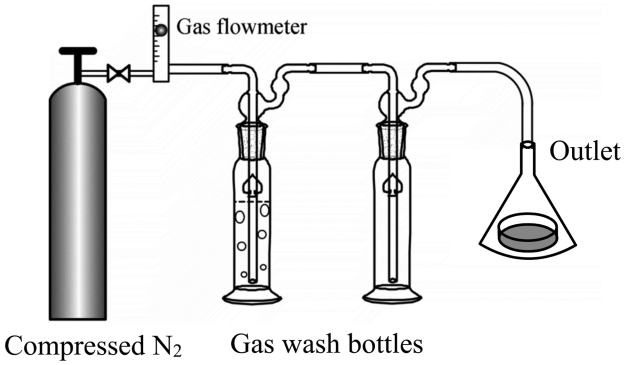

Breath Figure Patterns on a Glass Slide. A schematic representation of the experimental setup for the preparation of breath figure patterns on a glass slide is shown in Scheme 2. In a typical breath figure process, PS was dissolved in chloroform with a 6% (mass fraction) initial polymer concentration; 100 μL of the solution was then cast onto a glass slide using a microinjector. When the slide was placed in a stream of water-saturated air, the humidity of the air flow was maintained at 75% by controlling the flow rate. After solidification for 30 min, the film was dried at room temperature. In this way, breath figure was successfully patterned on a glass slide.

Measurement of the Remaining Solvent and the Amount of PS Dissolved. The solvent remaining and the amount of PS dissolved (W_d) in the solution were measured by weight. Typically, the solution was sampled from the substrates by dumping during the sDBF process. The solution was dried under vacuum at room temperature. The weight of the samples before and after drying was measured. If the condensing water was neglected in the solution, the weight loss of the sample was the solvent remaining in the solution. Accordingly, the weight of the samples after drying was the amount of PS dissolved (W_d) in the solution.

Cultivation of GFP Expressing *Escherichia coli* Cells in the PS Perti Dish. *E. coli* TG1 cells expressing green fluorescent protein (GFP) (using a pTrc99a vector) were cultivated following a protocol. The cells were inoculated in 10 mL of Luria-Bertani medium containing ampicillin (100 μg/mL) and cultivated for 17 h at 37 °C in a shaking incubator. This culture (50 μL) was used to inoculate 5 mL of TB medium in the PS Perti dish, supplemented with 100 μg/mL ampicillin and 1 mM IPTG. The cells were cultivated at 37 °C in a shaking incubator for 30 min or 3 h. The cells were harvested by centrifugation. The cells were washed with 1 mL of phosphate-buffered saline (pH 6.8, 0.1 M) and collected by centrifugation. The cell concentration in the last washing solution was tested. After removal of the cells in the solution by dumping, the honeycomb-structured PS Perti dish was gently washed with 1 mL of PBS buffer (twice). The honeycomb structures attached to GFP-expressing *E. coli* cells were observed using fluorescence microscopy.

RESULTS AND DISCUSSION

For practical applications, it is needed to control the surface morphology of the breath figure patterns. Here, we present a sample way to pattern breath figure with different surface morphology by adjusting the relative humidity (RH) during the sDBF process. As shown in Scheme 1, in the presence of moisture with a forced flow of air across the solution (chloroform-containing polymers), ordered honeycomb-like patterns could be formed on the PS or PMMA substrate by the evaporation of the volatile solvent. In the sDBF process, chloroform evaporated very fast and the surface of the solution

was cooled quickly, resulting in the nucleation and growth of water droplets on the PS or PMMA substrate. After a total evaporation of the chloroform and water, an ordered honeycomb-like structure was patterned on the surface of the polymeric substrate. The honeycomb-like substrates patterned under RHs of >90, 85, 75, 65, and 50% were named sDBF-90, sDBF-85, sDBF-75, sDBF-65, and sDBF-50, respectively. The surface morphology of the breath figure patterns was observed by scanning electron microscopy (SEM). Panels a and b of Figure 1 show that, under a really high RH (>90%), irregular

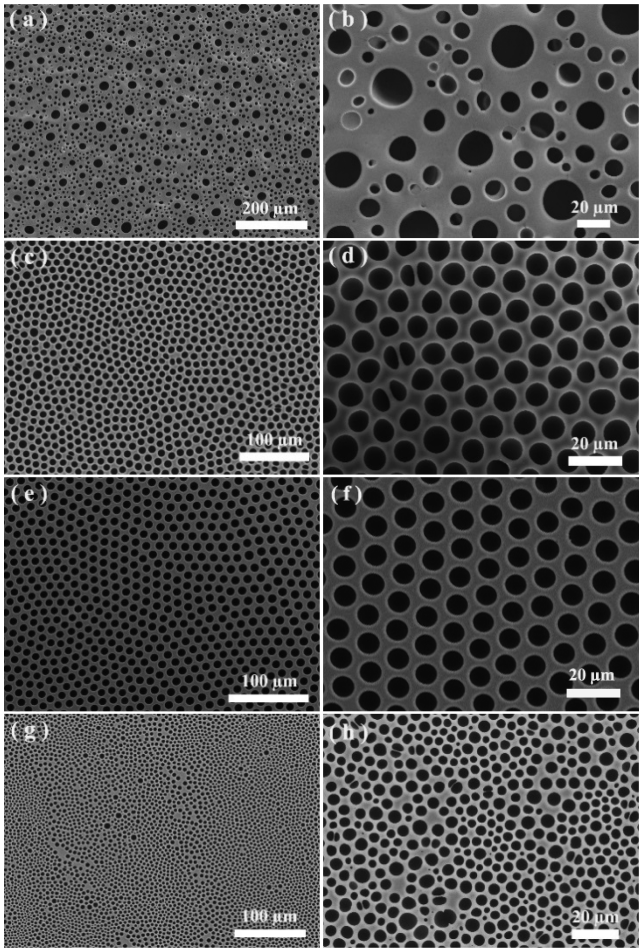

Figure 1. SEM images of breath figure patterns at low (a, c, e, and g) and high (b, d, f, and h) magnifications under different values of RH: (a and b) >90%, (c and d) 85%, (e and f) 75%, and (g and h) 65%. During the synthesis, 1 mL of chloroform was added to the Petri dish (3.5 cm in diameter).

pores were generated by sDBF. When the values of RH were decreased to 85%, a honeycomb-like structure was observed after evaporation of chloroform and water. However, approximately 5% of the pores were semicircular among the patterns (Figure 1c,d). When the value of RH was set at 75%, a well-ordered porous structure was shown during the breath figure patterns (Figure 1e,f). With a further decrease in the RH to 65%, the coalescence of the condensed water droplets is shown in panels g and h of Figure 1. It is noted that only pale traces were observed on the substrate after complete evaporation of the solvent when the RH was decreased to 50% (Figure S1 of the Supporting Information). The number-averaged diameter of the pores (D_n) on the PS substrate under different RHs is summarized in Figure 2b. Although there was correlation in the breath figure patterns, the pore diameter (D_n) on the PS substrate was increased (from 3.65 ± 0.43 to 11.21 ± 6.74 μm) with the enhancement of the humidity in general. This finding greatly agreed with the result reported by Park and Kim.[19] Hence, the surface morphology patterned on the substrates could be controlled by the RH during the sDBF process, and an ordered array of micrometer-sized pores (D_n = 7.9 ± 0.02 μm) could be achieved on sDBF-75.

The reason for the coalescence induced by the rapidly condensing water droplets at high RHs was demonstrated by investigating the physicochemistry parameters during the sDBF process.[16] It is known that the viscosity of the system affects the coalescence of the condensing water droplets. However, the viscosity of the solution was not homogeneous from the surface to the bottom. To generally indicate the viscosity of the solution, the solvent remained in the solution and the amount of PS dissolved (W_d) in the solution was measured by weight (see the Supporting Information). In a typical sDBF process (75% RH), the solvent remained and the W_d in the solution was studied, as shown in Figure 2a. On the basis of the solvent remaining and the W_d in the solution, the solution viscosity was calculated (Figure S2 of the Supporting Information). It is shown that the W_d in the solution increased rapidly, generally indicating the solution viscosity increased during solvent evaporation. When the polymer solution attained a certain viscosity value, the solution was changed into a nonflow state. Hence, the solvent in the breath figure system at different times was measured to determine the time for the formation of the nonflow state ($t_{non\text{-}flow}$). The values of $t_{non\text{-}flow}$ under different RHs are summarized in Figure S3 of the Supporting Information, which indicates a lower RH resulted in a larger $t_{non\text{-}flow}$. To show the effect of RH on viscosity, the W_d in the solution at the half-time of $t_{non\text{-}flow}$ ($t_{1/2non\text{-}flow}$) was measured. It is seen in Figure 2b that the W_d in the solution at $t_{1/2non\text{-}flow}$ was reduced when the RH was increased. At the same time, the D_n on the PS substrates was increased. These experiments indicate that the formation of the BF was affected by the RH in terms of both vapor pressure and viscosity of the solution. On one hand, the vapor pressure of the solvent (controlled by RH) heavily influences the structure of the breath figure.[20] Generally, a low air flow rate (50% RH) results in slower evaporation and a smaller decrease in the temperature on the surface of the solvent. Thus, a low air flow rate would lead to a low level of nucleation and growth of water droplets on the substrate (see Figure S1 of the Supporting Information). When the air flow rate is too high (>90% RH), the solvent evaporates too fast; therefore, the water droplets would condense onto the surface with insufficient time to arrange in a regular order (see Figure 1a).[21] On the other hand, the viscosity of the system affected the coalescence of the condensing water droplets. (i) A low viscosity resulted in disordered pattern arrays because of the coalescence of the water droplets. (ii) In a solution with a high viscosity, it is difficult for the water droplets to diffuse across the interface, leading to fewer and larger pores on the substrate. Regardless, we can generate an ordered array of breath figure on the substrate by integrating the vapor pressure and viscosity. The honeycomb structures obtained would lead to the substrates being suitable as scaffolds for tissue engineering in the molecular biology lab.

There are two main advantages to the sDBF method presented here. The first one is that the obtained honeycomb layer was indeed part of the substrate, which provides the

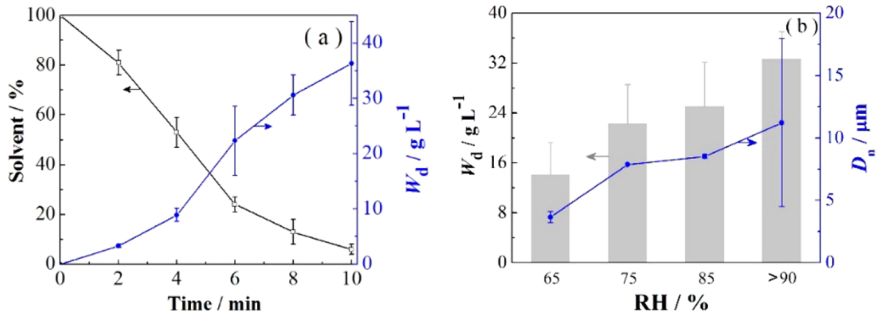

Figure 2. (a) Solvent remaining (vs the total amount of solvent) and amount of PS dissolved (W_d) in a typical sDBF process (75% RH). (b) W_d at $t_{1/2non\text{-}flow}$ and diameter of the pores (D_n) on a PS Petri dish under different RHs.

honeycomb structure with enough mechanical strength during the practical applications. To confirm this, a breath figure was patterned onto a glass slide (BF-patterned glass slide) using an NBF method. Both of the BF-patterned glass slides and the honeycomb-structured substrates were placed into an oven at 37 °C for 36 h. After this treatment, damage to the film (Figure 3a) with cracks on the walls between the cavities (Figure 3b)

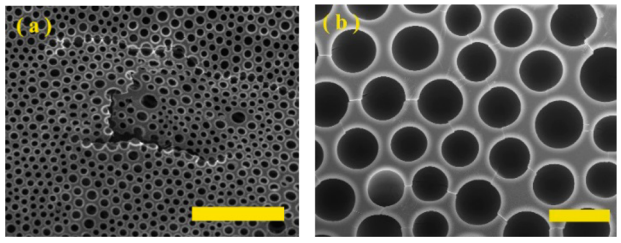

Figure 3. SEM images of breath figure patterns on a glass slide after a treatment at 37 °C for 36 h. The scale bars are 100 and 20 μm for panels a and b, respectively.

was clearly observed on the BF-patterned glass slide. However, no change was found on the surface morphology of the honeycomb-structured substrate after the same treatment. These experiments indicate the honeycomb structures on the Petri dish were much more stable than the breath figure on the glass slide.

The second advantage is that large-area and ordered honeycomb structure could be created on the substrate (e.g., Petri dish) because the polymer solution is free in this method. In an NBF method, a casting of the polymeric solution and another substrate were needed.[22] The repulsion between the polymer and the substrate during polymer drying would not only decrease the mechanical stability of the film but also limit the formation of large-area honeycomb structures via this traditional method. Therefore, it is still a challenge to obtain large-area and ordered honeycomb structure by an NBF process.[23−25] In the sDBF method presented here, the polymer solution is free and the repulsion between the polymer and the substrate can be neglected, which allows the direct patterning of large-area honeycomb structures onto a polymeric substrate (e.g., PS and PMMA). In the experiments described above, a PS Perti dish with a diameter of 3.5 cm was used. Hence, the area of the honeycomb structures was calculated to be 9.6 cm^2 (see Figure S7 of the Supporting Information). To confirm that this new method can generate large-area honeycomb structures on other Petri dishes, amplification experiments were conducted on a PMMA Petri dish (which was cut into 5 cm × 3 cm plates). From the pattern of honeycomb structures on the 15 cm^2 of the PMMA substrate, 1.5 mL of chloroform and a RH value of 75% were selected. The images in Figure 4 indicate

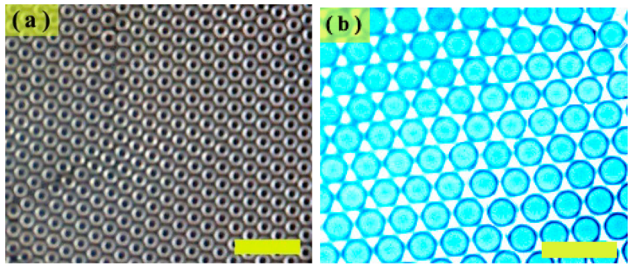

Figure 4. (a) Optical and (b) fluorescence microscope images of the honeycomb-structured PMMA substrate obtained via the sDBF method. The scale bars are 20 and 10 μm for panels a and b, respectively.

that a large-area hexagonal array could be directly patterned on the PMMA substrate. The D_n of the honeycomb pores on the PMMA substrate (4.1 ± 0.02 μm) was smaller and more uniform than that on the PS substrate, which might be due to the different dissolving and swelling capabilities between PS and PMMA in chloroform.

In a modern bacteriological laboratory, cell culture is at the heart of almost every experiment because it is an important way to obtain the source of the protein, RNA, and the genomic DNA sample. However, as molecular biology has expanded into more and more complex systems, there is a growing need to consider the natural environments in which the cells are grown.[26] In this case, modern Petri dishes garnered great interest worldwide because they could provide a three-dimensional (3D) environment where cells can behave as they do *in vivo*.[27,28] For example, using a 3D Petri dish with a honeycomb pattern, an artificial human ovary has been created with self-assembled human theca and granulosa cell micro-tissues and used for IVM and future oocyte toxicology studies.[29] This approach is one of the most promising developments in fertility medicine in recent memory, and it was hailed as one of TIME Magazine's "Top 10 Medical Breakthroughs" in 2010.[30] Therefore, it is a great challenge to fabricate the 3D Petri dishes in an easy and cheap way. In this work, the sDBF process was proposed to directly generate honeycomb-patterned Petri dishes to make 3D systems more flexible.

The porosity of the honeycomb Petri dish would influence cell attachment.[31−34] Unlike the flat Petri dish in which cells were grown or attached as a thin layer on the surface of the Petri dish, the honeycomb-structured Petri dish produced 3D-

enhanced aggregation of cells.[35,36] Therefore, the attachment of cells (*E. coli* TG1 cells expressing green fluorescent protein) on the honeycomb-patterned PS Petri dish (in comparison to a flat-bottomed PS culture dish) was investigated in this work. Table 1 displays the attachment of cells with different lengths of time. It is seen that weak attachment was found on the flat Petri dish (Table 1), while the honeycomb-structured Petri dish permitted the attachment of cells in the ordered cavities (Table 1 and Figure 5), indicating an increase in the surface area of the substrate via a honeycomb pattern improved the adhesion of cells onto the Petri dish.

Table 1. Cell Attachment and Cell Growth with Different Lengths of Time

experiment	Petri dish	30 min (cells/cm^2)	3 h (cells/cm^2)	ratio[a]
attachment	flat-bottomed	389	656	1.7
	sDBF-65	774	2953	3.8
	sDBF-75	691	2124	3.1
	sDBF-85	657	1918	2.9
growth	flat-bottomed	3749	9360	2.5
	sDBF-65	3045	10 210	3.4
	sDBF-75	2927	9749	3.3
	sDBF-85	2863	8892	3.1

[a]Ratio of the number of cells at 3 h to the number at 30 min.

Moreover, it was found that part of honeycomb cavities was empty after a short incubation (30 min), suggesting the interaction between cells is also important in the attachment. More interestingly, it was seen that the number of attached cells increased rapidly as the incubation time increased (Figure 5a–c) and most cells were aggregated in the porous cavities (Figure 5d). This experiment indicates that we can separate cells into divided aggregation using a simple incubation, which shows great potential in a future biosensor or bioreactor study.

Cell growth under different conditions is also shown in Figure 6 and Table 1. Cell growth after 30 min in Figure 6 shows the growth began from the honeycomb cavities. It is due to the fact that the honeycomb patterns improved the adhesion of cells onto the Petri dish. When the growth time was increased, the cells grew outside the honeycomb cavities. By testing the OD of the cells after a 3 h culture, we found the rate of cell growth on the honeycomb-patterned Petri dish to slightly increase compared to that on a flat-bottomed PS tissue culture. In addition, the rate of cell growth after 3 h on a Petri dish (sDBF-65, 3.4 times) with a pore size of 3.65 μm was higher than that on a Petri dish (sDBF-85, 3.1 times) with a pore size of 8.52 μm. These results indicate that the proliferation of cells was superior on the honeycomb-patterned Petri dish, perhaps because the honeycomb patterns provided a multiple-dimension environment in which cells could behave as they do *in vivo*.

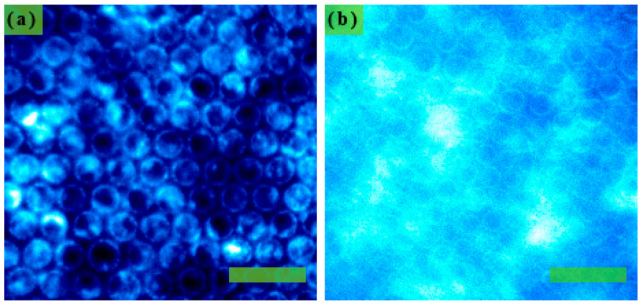

Figure 6. Fluorescence microscope images of cell growth on the honeycomb-structured Petri dish (sDBF-75) after a culture of (a) 30 min or (b) 3 h. The scale bar is 20 μm for both images.

CONCLUSIONS

In this work, we have proposed a simple breath figure method to directly prepare ordered honeycomb structures on PMMA substrates or commercial PS Petri dishes. Because an external polymer solution was not needed in the sDBF method, the repulsion between the polymer and the substrate during polymer solidification was neglected, which enhanced the pattern of large-area and honeycomb structures. Moreover, the honeycomb structure is indeed part of the substrate, providing the honeycomb layer with enough mechanical stability. The breath figure method in this work for the synthesis of the honeycomb structure is extremely simple with scale-up capability to large-area production, which offers new insights into surface engineering with great potential for use in commercial technologies.

ASSOCIATED CONTENT

Supporting Information

Optical images, SEM image, fluorescence images, and attachment of cells to the Petri dish. This material is available free of charge via the Internet at http://pubs.acs.org.

AUTHOR INFORMATION

Corresponding Author

*E-mail: xtshenlab@gmail.com or xiantao.shen@tbiokem.lth.se.

Notes

The authors declare no competing financial interest.

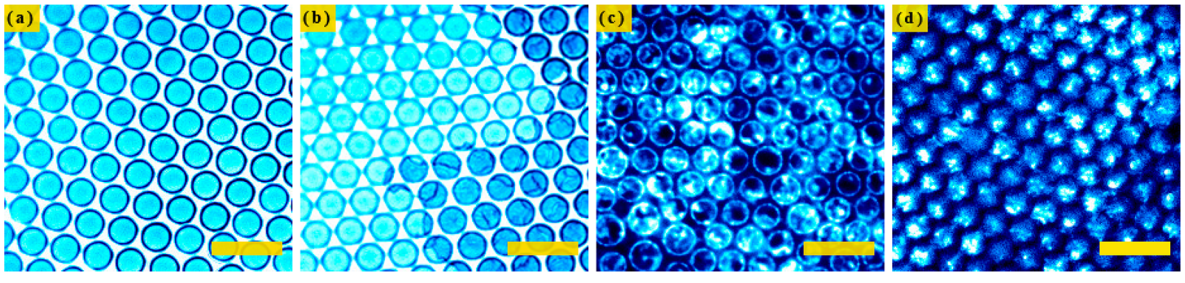

Figure 5. Fluorescence microscope images of the attachment of cells to the honeycomb-structured Petri dish (sDBF-75) after incubation for (a) 0 min, (b) 30 min, (c) 3 h, and (d) 3 h. Panel d is focused on cell aggregation in the honeycomb cavities. The initial optical density (OD_{600}) is 0.2 for the cell solution, and the scale bar is 20 μm for all images.

REFERENCES

(1) Davis, M. E. Ordered Porous Materials for Emerging Applications. *Nature* **2002**, *417*, 813−821.
(2) Zhang, H. Controlled/"Living" Radical Precipitation Polymerization: A Versatile Polymerization Technique for Advanced Functional Polymers. *Eur. Polym. J.* **2013**, *49*, 579−600.
(3) Nie, Z.; Kumacheva, E. Patterning Surfaces with Functional Polymers. *Nat. Mater.* **2008**, *7*, 277−290.
(4) Wu, D.; Xu, F.; Sun, B.; Fu, R.; He, H.; Matyjaszewski, K. Design and Preparation of Porous Polymers. *Chem. Rev.* **2012**, *112*, 3959−4015.
(5) Park, J. S.; Lee, S. H.; Han, T. H.; Kim, S. O. Hierarchically Ordered Polymer Films by Templated Organization of Aqueous Droplets. *Adv. Funct. Mater.* **2007**, *17*, 2315−2320.
(6) Lee, S. H.; Park, J. S.; Lim, B. K.; Mo, C. B.; Lee, W. J.; Lee, J. M.; Hong, S. H.; Kim, S. O. Highly Entangled Carbon Nanotube Scaffolds by Self-Organized Aqueous Droplets. *Soft Matter* **2009**, *5*, 2343−2346.
(7) Lee, S. H.; Lee, D. H.; Lee, W. J.; Kim, S. O. Tailored Assembly of Carbon Nanotubes and Graphene. *Adv. Funct. Mater.* **2011**, *21*, 1338−1354.
(8) Bunz, U. H. F. Breath Figures as a Dynamic Templating Method for Polymers and Nanomaterials. *Adv. Mater.* **2006**, *18*, 973−989.
(9) Bai, H.; Du, C.; Zhang, A.; Li, L. Breath Figure Arrays: Unconventional Fabrications, Functionalizations, and Applications. *Angew. Chem., Int. Ed.* **2013**, *52*, 12240−12255.
(10) Yu, Y.; Ma, Y. Breath Figure Fabrication of Honeycomb Films with Small Molecules through Hydrogen Bond Mediated Self-Assembly. *Soft Matter* **2011**, *7*, 884−886.
(11) Srinivasarao, M.; Collings, D.; Philips, A.; Patel, S. Three-Dimensionally Ordered Array of Air Bubbles in a Polymer Film. *Science* **2001**, *292*, 79−83.
(12) Stenzel-Rosenbaum, M. H.; Davis, T. P.; Fane, A. G.; Chen, V. Porous Polymer Films and Honeycomb Structures Made by the Self-Organization of Well-Defined Macromolecular Structures Created by Living Radical Polymerization Techniques. *Angew. Chem., Int. Ed.* **2001**, *40*, 3428−3432.
(13) Hoa, M. L. K.; Lu, M.; Zhang, Y. Preparation of porous materials with ordered hole structure. *Adv. Colloid Interface Sci.* **2006**, *121*, 9−23.
(14) Gau, H.; Herminghaus, S. Ripening of Ordered Breath Figures. *Phys. Rev. Lett.* **2000**, *84*, 4156−4159.
(15) Böker, A.; Lin, Y.; Chiapperini, K.; Horowitz, R.; Thompson, M.; Carreon, V.; Xu, T.; Abetz, C.; Skaff, H.; Dinsmore, A. D.; Emrick, T.; Russell, T. P. Hierarchical Nanoparticle Assemblies Formed by Decorating Breath Figures. *Nat. Mater.* **2004**, *3*, 302−306.
(16) Hernández-Guerrero, M.; Stenzel, M. H. Honeycomb Structured Polymer Films *via* Breath Figures. *Polym. Chem.* **2012**, *3*, 563−577.
(17) Farbod, F.; Pourabbas, B.; Sharif, M. Direct Breath Figure Formation on PMMA and Superhydrophobic Surface Using In Situ Perfluoro-Modified Silica Nanoparticles. *J. Polym. Sci., Part B: Polym. Phys.* **2013**, *51*, 441−451.
(18) Wan, L.; Ke, B.; Li, X.; Meng, X.; Zhang, L.; Xu, Z. Honeycomb-Patterned Films of Polystyrene/Poly(ethylene Glycol): Preparation, Surface Aggregation and Protein Adsorption. *Sci. China, Ser. B: Chem.* **2009**, *52*, 969−974.
(19) Park, M. S.; Kim, J. K. Breath Figure Patterns Prepared by Spin Coating in a Dry Environment. *Langmuir* **2004**, *20*, 5347−5352.
(20) Megelski, S.; Stephens, J. S.; Chase, D. B.; Rabolt, J. F. Micro- and Nanostructured Surface Morphology on Electrospun Polymer Fibers. *Macromolecules* **2002**, *35*, 8456−8466.
(21) Stenzel, M. H.; Barner-Kowollik, C.; Davis, T. P. Formation of Honeycomb-Structured, Porous Films via Breath Figures with Different Polymer Architectures. *J. Polym. Sci., Part A: Polym. Chem.* **2006**, *44*, 2363−2375.
(22) Widawski, G.; Rawiso, M.; François, B. Self-Organized Honeycomb Morphology of Star-Polymer Polystyrene Films. *Nature* **1994**, *369*, 387−389.
(23) Park, M. S.; Kim, J. K. Broad-Band Antireflection Coating at Near-Infrared Wavelengths by a Breath Figure. *Langmuir* **2005**, *21*, 11404−11408.
(24) Chen, P.-C.; Wan, L.-S.; Ke, B.-B.; Xu, Z.-K. Honeycomb-Patterned Film Segregated with Phenylboronic Acid for Glucose Sensing. *Langmuir* **2011**, *27*, 12597−12605.
(25) Lomoschitz, M.; Edinger, S.; Bauer, G.; Friedbacher, G.; Schubert, U. Sol−Gel Films with Polymodal Porosity by Surfactant-Assisted Breath Figure Templating. *J. Mater. Chem.* **2010**, *20*, 2075−2078.
(26) Deans, T. L.; Singh, A.; Gibson, M.; Elisseeff, J. H. Regulating Synthetic Gene Networks in 3D Materials. *Proc. Natl. Acad. Sci. U.S.A.* **2012**, *109*, 15217−15222.
(27) Zhang, S. Beyond the Petri Dish. *Nat. Biotechnol.* **2004**, *22*, 151−152.
(28) Napolitano, A. P.; Dean, D. M.; Man, A. J.; Youssef, J.; Ho, D. N.; Rago, A. P.; Lech, M. P.; Morgan, J. R. Scaffold-Free Three-Dimensional Cell Culture Utilizing Micromolded Nonadhesive Hydrogels. *BioTechniques* **2007**, *43*, 494−500.
(29) Krotz, S. P.; Robins, J. C.; Ferruccio, T.-M.; Moore, R.; Steinhoff, M. M.; Morgan, J. R.; Carson, S. In Vitro Maturation of Oocytes via the Pre-Fabricated Self-Assembled Artificial Human Ovary. *J. Assisted Reprod. Genet.* **2010**, *27*, 743−750.
(30) http://www.time.com/time/specials/packages/article/0,28804,2035319_2034529_2034518,00.html.
(31) Beattie, D.; Wong, K. H.; Williams, C.; Poole-Warren, L. A.; Davis, T. P.; Barner-Kowollik, C.; Stenzel, M. H. Honeycomb-Structured Porous Films from Polypyrrole-Containing Block Copolymers Prepared via RAFT Polymerization as a Scaffold for Cell Growth. *Biomacromolecules* **2006**, *7*, 1072−1082.
(32) Wu, X.; Wang, S. Regulating MC3T3-E1 Cells on Deformable Poly(ε-caprolactone) Honeycomb Films Prepared Using a Surfactant-Free Breath Figure Method in a Water-Miscible Solvent. *ACS Appl. Mater. Interfaces* **2012**, *4*, 4966−4975.
(33) Nishikawa, T.; Nishida, J.; Ookura, R.; Nishimura, S. I.; Wada, S.; Karino, T.; Shimomura, M. Honeycomb-Patterned Tthin Films of Amphiphilic Polymers as Cell Culture Substrates. *Mater. Sci. Eng., C* **1999**, *8*−*9*, 495−500.
(34) Zhao, W.; Lang, M.; Li, Y.; Li, L.; Shi, J. Robust and Hydrophilic Polymeric Films with Honeycomb Pattern and Their Cell Scaffold Applications. *J. Mater. Chem.* **2009**, *19*, 2789−2796.
(35) Lee, J.; Cuddihy, M. J.; Kotov, N. A. Three-Dimensional Cell Culture Matrices: State of the Art. *Tissue Eng., Part B* **2008**, *14*, 61−86.
(36) Zhang, S.; Gelain, F.; Zhao, X. Designer Self-Assembling Peptide Nanofiber Scaffolds for 3D Tissue Cell Cultures. *Semin. Cancer Biol.* **2005**, *15*, 413−420.